UC Berkeley
UC Berkeley Previously Published Works

Title

Effects of Solvents on the Electrochemical Performance of LiFePO4/C Composite Electrodes

Permalink

Journal

ISSN

Authors

Wang, Guixin
Kang, Hanchang
Chen, Miao
et al.

Publication Date

DOI

Influence of electrolytes on the low-temperature performance of LiFePO₄/C composite electrodes

Guixin Wang [1,*], Hanchang Kang [1], Miao Chen [1], Kangping Yan [1], Xueshan Hu [2], Elton J. Cairns [3,4]

[1] *College of Chemical Engineering, Sichuan University, Chengdu 610065, Sichuan, China*

[2] *BASF Battery Materials (Suzhou) Co., Ltd., Suzhou Industrial Park, Suzhou 215123, Jiangsu, China*

[3] *Department of Chemical and Biomolecular Engineering, University of California, Berkeley, CA, USA,*

[4] *Environmental Energy Technologies Division, Lawrence Berkeley National Laboratory, Berkeley, CA, USA*

ABSTRACT

The electrolyte, a key cell component for the successful operation of electrode materials, is greatly affected by its solvents. The influence of nonaqueous solvents on the electrochemical performance of a LiFePO₄/C composite cathode was investigated at various operating temperatures. The kinetics of the LiFePO₄/C composite electrode reaction, including changes of rate capability, redox potential, polarization degree, electrode reaction process, lithium ion diffusion efficiencies, exchange current densities, and activation energies, were evaluated using various techniques. The composition and composition ratio of solvents greatly affect the electrode reaction kinetics. In the mixed solvents of ethylene carbonate (EC), dimethyl carbonate (DMC) and ethyl methyl carbonate (EMC), EMC is beneficial for the room temperature performance, while the substitution of 20 vol.% of EMC by ethyl acetate (EA) is good for the low temperature performance. When 30 vol.% of DMC is substituted by 10

* Corresponding author.
E-mail address: guixin66@scu.edu.cn, guixinwang1@gmail.com
Tel.: +86-28-85406192.

vol.% of EMC and 20 vol.% of EA, the diffusion coefficient of lithium ions increases from 2.62×10^{-12} to 2.50×10^{-11} cm^2 s^{-1}, while the exchange current density increases from 2.20×10^{-5} to 3.75×10^{-5} A cm^{-2} at -20 ºC, and the activation energy of the electrode reaction decreases from 48.36 to 33.01 kJ mol^{-1}. These results are significant for the exploration of appropriate electrolytes for the extensive applications of LiFePO$_4$/C composite electrodes.

1. INTRODUCTION

The serious environmental problems encourage the use of (hybrid) electric vehicles in cities, and energy materials are necessary for the vehicle power sources operating at different ambient temperatures. Among various positive electrode materials, olivine-structured $LiFePO_4$ has attracted considerable interest because of its unique structure, good thermal stability, plentiful raw material supply, and environmental compatibility [1], but the low-temperature performance must be improved for its practical application in different environments [2-6]. Low-temperature cell performance is strongly influenced by electrolyte composition, electrode material composition and battery structure. Current studies on the enhancement of the low-temperature performance of $LiFePO_4$ focus on doping elements [7], carbon coating [8, 9], or using quaternary electrolytes with specific formulations [3, 10].

As the blood of batteries, the electrolyte will affect the transport properties of Li^+ ions [11-13] as well as the solid interface film on the electrodes, and the solvent plays an important role in determining cell performance [13]. The solvent affects the transfer processes of mass, heat, momentum, and charge by forming different solvated ions and altering the physical properties of the electrolyte, such as the melting point, viscosity, solubility, and conductivity. Many solvents, including EC, DMC, EMC and EA, have been employed to enhance the performance of Li ion cells for different applications. Among these solvents, EC is frequently used because it is aprotic, polar, and non-volatile [13-18]; DMC can improve the solubility and conductivity of the electrolyte because of its relatively higher dielectric

constant and low viscosity [13, 15]; EMC is a useful co-solvent to widen the liquid range and to enhance the conductive behavior of the EC-based electrolytes [13, 17-21]; and EA can improve ionic transport properties in a solution [13, 22, 23]. The solvent mixture is of great significance for improving the electrochemical performance of electrolytes. A ternary electrolyte of 1.0 M $LiPF_6$/EC + DMC+ EMC (1: 1: 1) is reported to enhance the low-temperature performance of $LiCoO_2$ [24], and a quaternary electrolyte of $LiPF_6$/EC + DEC + DMC + EMC is found to improve the low-temperature performance of $LiNi_{0.8}Co_{0.2}O_2$ [25]. However, the influence of the type and combination of solvents on the low-temperature performance of $LiFePO_4$ is still unclear, which is not beneficial for its extensive application.

Herein, three types of $LiPF_6$ electrolytes containing different solvents were chosen and compared for improving the electrochemical performance of $LiFePO_4$/C composite electrodes using various techniques at different cell operating temperatures. The electrode reaction process was analyzed, and the functions of the various solvents were discussed, which is important for the compatibility of electrode materials and electrolytes.

2. EXPERIMENTAL

2.1 Materials

In order to decrease the cost and realize sustainable development, a $LiFePO_4$/C composite was

synthesized with a facile route by using Fe$_{1.5}$P waste slag from the industrial production of yellow phosphorus [26]. Three types of electrolytes containing different solvents, denoted as "1", "2" and "3", were provided by BASF Battery Materials (Suzhou) Co., Ltd. These electrolytes are all composed of 1.0 M LiPF$_6$ and 2 wt.% of vinylene carbonate (VC) additive, along with different solvents like EC, DMC, EMC and EA, and the detailed compositions are shown in Table 1. The key physicochemical properties of each solvent are summarized in Table 2. Electrolytes "1" and "2" are ternary systems of EC+DMC+EMC with different ratios of DMC and EMC, while electrolyte "3" is a quaternary system with part of the EMC substituted by EA to decrease the melting point and increase the conductivity of the electrolyte.

2.2 Characterization

The phase structures of the synthesized sample were identified by X-ray diffraction (XRD, Philips X'Pert Pro, Netherlands) with a step of 0.04º/s within the 2θ range from 10º to 70º using Cu Kα radiation at a power of 40 kV×100 mA. The morphology and the particle size were observed using a field-emission scanning electron microscope (FESEM, JSM-7500F, Japan). The carbon content was determined by a carbon-sulfur analyzer (CS-902, China).

2.3 Electrochemical evaluation

The electrochemical measurements were conducted on CR2032 coin cells at different temperatures. The cathodes were composed of 80 wt.% of the as-synthesized LiFePO$_4$/C powder, 15 wt.% of

conductive acetylene black and 5 wt.% of commercial LA-132 binder (Chengdu Indigo Power Sources

Co. Ltd, China). Lithium metal was used as the anode, acting as the counter and reference electrode.

Using the above various electrolytes, cells were assembled by sandwiching a Celgard 2300

microporous separator between the cathode and the anode in a glove box filled with dry argon gas [26, 27].

   The electrochemical performance of the cells was evaluated via galvanostatic charge/discharge

curves, cyclic voltammetry (CV) and electrochemical impedance spectroscopy (EIS). The galvanostatic

charge/discharge tests were performed in a potential range of 2.4 ~ 4.2 V versus Li^+/Li on a Neware

battery-testing instrument (Shenzhen Neware Technology Ltd., China). CV and EIS measurements

were carried out on an electrochemical station including a PAR 273A potentiostat/galvanostat and a

signal recovery model 5210 lock-in-amplifier controlled by Powersuite software (Princeton Applied

Research, USA). The potential window for the CVs is the same for the above galvanostatic tests. As for

the EIS measurements, the AC signal amplitude is 10 mV, and the frequency range is between 100 kHz

and 0.01 Hz. The lithium ion diffusion coefficient (D_{Li}) is calculated according to the function of the

impedance and the square root of frequency in the low frequency region of the EIS data. According to

the exchange current density at different temperatures, the activation energies of the Li^+ electrode

reaction are calculated by using the Arrhenius equation.

3. RESULTS AND DISCUSSION

3.1 Phase structure and morphological analysis

After being well mixed by ball milling, the precursor was preheated at 500 ~ 550 ºC in air, and then calcined at ~700 ºC in argon [26]. Finally, a black product was obtained and ground for further analysis. According to the carbon-sulfur analysis, the carbon content is about 5 wt.%. In order to determine the composition and phase structure, powder XRD was conducted. From the XRD pattern in Figure 1, all the indexed peaks match well with the standard peaks of $LiFePO_4$ (JPCDS card number 40-1499), indicating the product is olivine $LiFePO_4$ with an orthorhombic structure and a Pmnb space group. The absence of impurity peaks indicates that the purity of the product is high. Via Rietveld refinement, the lattice parameters along the axes of a, b, and c are 0.60, 1.04 and 0.47 nm, respectively, and the cell volume is 0.29 nm^3. Among the indexed peaks, four main peaks centered at $2\theta \approx 20.8°$, $25.5°$, $29.7°$, and $35.5°$, can be attributed to the (011), (111), (121), and (131) crystal planes of $LiFePO_4$, respectively. The average crystallite size is 46.6 nm by calculating from these main planes using Scherrer's formula [27].

The SEM images in Figure 2 show that the as-synthesized $LiFePO_4$/C composite consists of many small quasi-spherical particles. Part of these particles agglomerate to form larger ones, while some small particles distribute among and on the surface of some large particles. The small particle size is in the the range of 15 to 30 nm, and the agglomeration size can reach 200 nm.

3.2 Charge/discharge performance

Typical galvanostatic charge/discharge curves of the CR2032 lithium cells using various electrolytes at the 0.1 C rate at different temperatures are shown in Figure 3. The composition and ratio of solvents greatly affect the charge/discharge behavior of $LiFePO_4$/C composite under the same conditions. Some key parameters, including discharge capacity, columbic efficiency (η), intermediate voltage difference between the charge and discharge plateaus (ΔV), are summarized in Table 3. As temperature decreases from 20 ºC to -20 ºC, the charge/discharge plateaus become shorter, the capacity declines, and the ΔV increases, indicating that the overvoltage increases at low temperatures. Electrolytes "1" and "2" without EA deliver better performance than electrolyte "3" containing EA at 20 ºC, which is in contrast

to the results at 0 or -20 ºC. Electrolyte "2" and electrolyte "3" exhibits the highest discharge capacity and the lowest ΔV at 20 °C and -20 °C, respectively, suggesting that the internal resistance of the cell using electrolyte "3" is the lowest at low temperature. Furthermore, electrolyte "3" is superior to electrolytes "1" and "2" in enhancing the columbic efficiency at -20 °C, indicating that electrolyte "3" with the quaternary solvent mixture provides good capacity reversibility at low temperatures. Considering the composition and the electrochemical performance, EA is inferior to EMC for enhancing the performance at room temperature, but EA is superior to EMC at low temperatures. On the other hand, electrolytes "1" and "2" contain the same components except with different ratios between the solvents of EMC and DMC, but their performances differ greatly. Electrolyte "2" with a higher content of EMC extends the low temperature operation range, and is better than electrolyte "1" for enhancing the discharge capacity at both room temperature and low temperature, indicating that EMC is superior to DMC for improving the electrochemical performance of $LiFePO_4$/C composite over a wide temperature ange. The difference in discharge capacity may be mainly due to the different freezing points of EMC (-55 ºC) and DMC (4.6 ºC) which will affect the diffusion of lithium ions [13]. Electrolytes "2" and "3" contain the same ratio of EC and DMC except the different contents of EMC and EA. Electrolyte "2" with 0 vol.% of EA and 50 vol.% of EMC exhibits better performance than Electrolyte "3" with 20 vol.% of EA and 30 vol.% of EMC at 20 ºC. However, Electrolyte "2" exhibits poorer performance than Electrolyte "3" in enhancing the discharge capacity at low temperatures of 0 ºC or -20 ºC, indicating that EMC is superior to EA for enhancing the electrochemical performance of the $LiFePO_4$/C composite at room temperature, but EMC is inferior to EA for improve\ing the low-temperature performance.

Figure 4 shows the differential capacity plots of the data shown in Figure 3, which reflects the changes of potential dE with reaction time dt because of the constant current charge/discharge. They all have an obvious pair of symmetric anodic/cathodic peaks at various temperatures, indicating that the

reversibility of the oxidation/reduction process is high. When the temperature is at -20 °C, the curves of

the cell using Electrolyte "3" exhibit two pairs of small extra oxidation/reduction peaks (~4.2/2.8 V and

~3.8/3.1 V) besides the pair of obvious redox peaks (~3.5/3.4 V). However, these extra peaks disappear

when the temperature increases to 0 ºC or 20 ºC. Noticeably, no other extra peaks appear in the curves

of electrolytes "1" and "2" at any temperature. Considering the extra redox peaks and improved

discharge capacity of the LiFePO$_4$/C composite at -20 °C, EA in the electrolyte may take part in the

electrode reaction to enhance the low temperature performance.

Figure 5 shows the rate performance of the LiFePO$_4$/C composite at various temperatures as the rate

ranges from 0.1 to 1.0 C. It can be seen that the rate capability declines with the decrease of

temperature. At 20 ºC, e\Electrolyte "2" has the best rate performance, and the discharge capacities can

reach 144.9, 119.6, and 94.5 mAh g^{-1} when the rates are 0.1 C, 0.5 C, and 1.0 C, respectively. At 0 ºC,

Electrolyte "2" also has the best rate performance, and the discharge capacities are 98.9, 83.9, and 73.4

mAh g^{-1} when the rates are 0.1 C, 0.5 C, and 1.0 C, respectively. However, when the temperature is

decreased to -20 ºC, Electrolyte "3" has the best rate performance, and the discharge capacities can

reach 86.0, 61.1, and 52.0 mAh g^{-1} when the rates are 0.1 C, 0.5 C, and 1.0 C, respectively.

3.3 Voltammetric analysis

Figure 6 shows the cyclic voltammograms of the cells using different electrolytes with a scanning

rate of 0.2 mV s^{-1} at -20 °C. They all have a pair of obvious redox peaks, but the peak positions and

intensities differ greatly. The values of oxidization potential (E_O), reduction potential (E_R), potential difference between oxidization and reduction peaks (ΔE), oxidation peak current (I_O) and reduction peak current (I_R) are summarized in Table 4. The oxidization peak at ~3.75 V and the reduction peak at ~3.20 V correspond to the de-intercalation of Li^+ ions from $LiFePO_4$ and the intercalation of Li^+ ions into $FePO_4$, respectively. The electrolyte sequence for increasing values of ΔE of the cells is "1" > "2" > "3", indicating that the polarization of the cell using Electrolyte "3" is the lowest at -20 °C. Meanwhile, the electrolyte sequence for increasing values of I_O and I_R is "3" > "2" > "1", suggesting that electrolyte "3" has a higher electrochemical reaction activity than electrolyte "1" or "2" at -20 °C. These results, consistent with the above galvanostatic charge/discharge results, further confirm that EA is better than EMC and DMC for enhancing the electrochemical performance of the $LiFePO_4/C$ composite at -20 °C.

3.4 Impedance analysis

To investigate the electrode reaction kinetics and diffusion behavior of lithium ions using different electrolytes, EIS measurements were conducted under the same conditions with an open circuit potential of 3.44 V by charging at different temperatures. The Nyquist plots of the $LiFePO_4/C$ composite using different electrolytes, along with the equivalent circuit used for EIS data modeling are presented in Figure 7. Their shapes are similar, and all curves consist of a depressed semicircle in the high-to-medium frequency region and an oblique line in the low frequency region, suggesting a similar electrode reaction process. However, the impedance values are greatly affected by the electrolytes with different solvents. The intercept of the curve on the real axis in the high-frequency region is attributed to the ohmic resistance of the electrolyte, and the depressed semicircle in the high-to-medium

frequency range is related to the complex reaction process over the interface between electrode and electrolyte, including electrolyte film and charge transfer impedances [28]. The inclined line in the low frequency range is associated with the Warburg impedance, which is from the semi-infinite diffusion of Li^+ ions in the bulk electrode [26,28].

The EIS curves are well fitted with the R(QR)(Q(RW)) model provided in Figure 7(d). Considering the inhomogeneities such as porosity, roughness and geometry in the electrode system, a constant phase element (CPE) Q is used to substitute for capacitance, and its value is determined by frequency independent parameters related to temperature [29]. In the circuit, R_s, R_f, Q_f, R_{ct}, W, and Q_d correspond to the ohmic resistance of the electrolyte, the resistance of the electrolyte film, the CPE of the film, the charge transfer reaction resistance, the Warburg impedance, and the CPE of the electrolyte film/electrode interface, respectively. In order to make clear the function of solvents for the electrode reaction process, the fitting results of R_s, R_{ct} and R_f by using ZsimpWin and Z-view software are summarized in Table 5. The values of R_s, R_{ct} and R_f increase gradually as temperature decreases. When the temperature is at 20 °C, the resistance sequence of the electrolytes is "1" < "3" < "2", the resistance sequence of charge transfer is "1" < "2" < "3", and the resistance sequence of the electrolyte film is "3" < "2" < "1", indicating that EMC with higher content reduces the conductivity of electrolyte, but EMC and EA disturb the electrode reaction process. When the temperature decreases to 0 or -20 °C, the resistance sequence of the electrolytes is "1" < "2" < "3", and the resistance sequence of the electrolyte film is "3" < "1" < "2", but the resistance sequences of charge transfer are "1" < "3" < "2" and "3" < "2" < "1", respectively. These results show that DMC is beneficial for improving the electrolyte conductivity at room temperature and low temperatures, and EA is good for the charge transfer reaction and for decreasing the electrolyte film resistance at low temperatures, but EMC will hinder the charge transfer and increase the electrolyte film resistance at low temperatures.

The chemical diffusion coefficients of lithium ions D_{Li^+} (cm^2 s^{-1}) are calculated from the complex

plane using the following equations of (1) and (2) according to the Fick's law [30, 31].

$$Z_W = \sigma(1-i)\omega^{-1/2} \qquad\qquad (1)$$

$$D_{Li^+}^{1/2} = \frac{RT}{2^{1/2} n^2 F^2 A \sigma C_{Li^+}} \qquad\qquad (2)$$

Where, Z_W is Warburg impedance at low frequency, σ is the Warburg coefficient, $i = \sqrt{-1}$, ω is the

frequency, R is the gas constant (R = 8.314 J mol^{-1} k^{-1}), T is the working temperature (K), n is the

number of transferred electrons, F is the Faraday constant (F = 96500 C mol^{-1}), and A is the active

surface area, and C_{Li^+} (mol cm^{-3}) is the molar concentration of lithium ions in an electrode active

material. According to Equation (1), the Warburg coefficient σ can be obtained from the slope of

impedance versus square root of frequency in the Warburg section. Figure 8 exhibits the dependence of

impedance Z' on square root of low frequencies at various temperatures, and the values of σ are

summarized in Table 5. According to Equation (2), the chemical diffusion coefficients D_{Li^+} (cm^2 s^{-1})

using various electrolytes are compared in Figure 9. Under the same conditions, the different values of

D_{Li^+} are from the different electrolytes. At 20 ºC, the electrolyte sequence for increasing values of D_{Li^+}

is "1" < "3" < "2", but the sequence changes to "1" < "2" < "3" at low temperatures of 0 or -20 ºC,

indicating the sequence for enhancing the diffusivity of lithium ions is DMC < EA < EMC at room

temperature, while the sequence changes to DMC < EMC < EA at low temperatures.

To further evaluate the intrinsic rates of electron transfer between electrolyte and electrode at various temperatures, the exchange current density (j) was calculated using the above charge transfer resistance R_{ct} obtained from the modeling results of EIS data by the following formula [32].

$$j = \frac{RT}{nFR_{ct}A} \qquad (3)$$

Where, the meanings of parameters like R, T, n, F, A, are consistent with those in the Equations (1) and (2). To confirm more clearly the temperature effect on the electrode reaction, the apparent activation energy (E_a) of the electrode reaction was calculated using the conventional Arrhenius equation [33]

$$\ln j = \ln K - \frac{E_a}{RT} \qquad (4)$$

Where, K is a temperature-independent coefficient. The formula is further transformed to the following one according to different temperatures T_1 and T_2.

$$\ln \frac{j_2}{j_1} = \frac{E_a}{R}(\frac{T_2 - T_1}{T_1 T_2})$$

The exchange current densities of j at various temperatures and the average activation energy E_a obtained from the three temperatures are summarized in Table 6. According to the results, DMC is good for the electron transfer at 20 or 0 ºC, while EMC or EA does well for the electron transfer at -20 ºC. On the other hand, Electrolyte "1" with highest content of DMC and lowest content of EMC has the

highest *J*, while Electrolytes "2" and "3" with a higher content of EMC have a lower E_a, indicating that

EMC is superior to DMC to improve the extraction/insertion of lithium ions in the electrode reaction.

Furthermore, Electrolyte "3" with EA replacing some of the EMC has a slightly lower activation

energy than Electrolyte "2", which is indicative of an easier electrode reaction.

According to the composition and structure of the different solvents in the electrolytes, the

performance differences are due to the different solvents. EC has good properties for forming a

Solid/Electrolyte Interface (SEI) film and dissolving lithium salts, while VC is an ideal additive for

forming a film to enhance capacity and cycling performance, which are reasons for the addition of 30

vol.% of EC and 2 wt.% of VC to each electrolyte. Thus, other solvents and matching ratios are key

factors for affecting the electrochemical performance of electrode materials at various temperatures.

Based on the above analytical results and the physicochemical properties of the different solvents,

EMC is better than DMC for improving the discharge capacity and rate performance of the $LiFePO_4$/C

composite at various temperatures of 20, 0 and -20 ºC. In addition, EMC is superior to EA for

improving the discharge capacity and rate performance at room temperature, but EMC is inferior to EA

for enhancing the electrochemical performance at low temperatures of 0 and -20 ºC. Consequently, the

combination and content of solvents are significant for improving the electrochemical performance of

the $LiFePO_4$/C composite electrode material at different temperatures.

4. CONCLUSIONS

The type and ratio of solvents in a 1.0 M $LiPF_6$ electrolyte affect greatly the electrochemical performance of a $LiFePO_4$/C composite active material at different temperatures. The influene of the solvents on the electrode reaction kinetics has been discussed in detail. According to the experimental results using various techniques, EMC is superior to DMC for improving the electrochemical performance of a $LiFePO_4$/C composite at 20, 0 and -20 ºC, and EMC is better than EA for increasing the electrochemical performance at room temperature, but EMC is inferior to EA for enhancing the electrochemical performance at low temperatures of 0 and -20 ºC. On the other hand, DMC is beneficial for improving the electrolyte conductivity at room temperature or low temperatures, EA is good for the electrode reaction and for decreasing the electrolyte film resistance at low temperatures, and EMC will enhance the charge transfer and increase the SEI film resistance at low temperatures. The sequence for enhancing the diffusivity of lithium ions is DMC < EA < EMC at 20 ºC, while the sequence changes to DMC < EMC < EA at low temperatures of 0 and -20 ºC. The activation energies of the electrode reaction using electrolytes "1", "2" and "3" were calculated to be 48.36, 33.29 and 33.01 kJ mol^{-1}, respectively, indicating that the ability for improving the extraction/insertion of lithium ions is DMC < EMC < EA. The combination of EC: DMC: EMC (30: 20: 50 in volume) was demonstrated to enhance the room temperature performance, while the combination of EC: DMC: EMC: EA (30:20:30:20 in volume) is beneficial to the low temperature performance. The experimental

results are of great significance for exploring appropriate electrolytes using combined solvents for improving the electrochemical performance of the LiFePO$_4$/C composite to satisfy possible applications at different temperatures.

ACKNOWLEDGEMENTS

References:

1. Dunn, B.; Kamath, H.; Tarascon, J. Electrical energy storage for the grid: a battery of choices. *Science* **2011**, *334* (6058), 928-935.

2. Zhang, S. S.; Xu, K.; Jow, T. R. An improved electrolyte for the LiFePO$_4$ cathode working in a wide temperature range. *J. Power Sources* **2006**, *159* (1), 702-707.

3. Liao, X.; Ma, Z.; Gong, Q.; He, Y.; Pei, L.; Zeng, L. Low-temperature performance of LiFePO$_4$/C cathode in a quaternary carbonate-based electrolyte. *Electrochem. Commun.* **2008**, *10* (5), 691-694.

4. Wang, Y.; He, P.; Zhou, H. Olivine LiFePO$_4$: development and future. *Energ. Environ. Sci.* **2011**, *4* (3), 805-817.

5. Smart, M. C.; Ratnakumar, B. V.; Ryan-Mowrey, V. S.; Surampudi, S.; Prakash, G. K. S.; Hu, J.; Cheung, I. Improved performance of lithium-ion cells with the use of fluorinated carbonate-based electrolytes. *J. Power Sources* **2003**, *119-121* (0), 359-367.

6. Aurbach, D.; Talyosef, Y.; Markovsky, B.; Markevich, E.; Zinigrad, E.; Asraf, L.; Gnanaraj, J. S.; Kim, H. Design of electrolyte solutions for Li and Li-ion batteries: a review. *Electrochim. Acta* **2004**, *50* (2-3), 247-254.

7. Wu, B.; Zhang, Y.; Li, N.; Yang, C.; Yang, Z.; Zhang, C.; Wu, F. Research on Low Temperature Performance of the F-doped LiFePO4/C Cathode Materials. *Journal of new material for electrochemical systems* **2011**, *14* (3), 147-152.

8. Wang, J.; Sun, X. Understanding and recent development of carbon coating on LiFePO$_4$ cathode materials for lithium-ion batteries. *Energ. Environ. Sci.* **2012**, *5* (1), 5163-5185.

9. Zhou, Y.; Gu, C. D.; Zhou, J. P.; Cheng, L. J.; Liu, W. L.; Qiao, Y. Q.; Wang, X. L.; Tu, J. P. Effect of carbon coating on low temperature electrochemical performance of LiFePO$_4$/C by using polystyrene sphere as carbon source. *Electrochim. Acta* **2011**, *56* (14), 5054-5059.

10. Ravet, N.; Gauthier, M.; Zaghib, K.; Goodenough; Mauger, A.; Gendron, F.; Julien Mechanism of the Fe^{3+} Reduction at Low Temperature for LiFePO$_4$ Synthesis from a Polymeric Additive. *Chem. Mater.* **2007**, *19* (10), 2595-2602.

11. Lin, H. P.; Chua, D.; Salomon, M.; Shiao, H.; Hendrickson, M.; Plichta, E.; Slane, S. Low-Temperature Behavior of Li-Ion Cells. *Electrochem. Solid St.* **2001**, *4* (6), A71-A73.

12. McCloskey, B. D.; Bethune, D. S.; Shelby, R. M.; Girishkumar, G.; Luntz, A. C. Solvents' critical role in nonaqueous lithium-oxygen battery electrochemistry. *J. Phys. Chem. Lett.* **2011**, *2* (10), 1161-1166.

13. Xu, K. Nonaqueous liquid electrolytes for lithium-based rechargeable batteries. *Chem. Rev.* **2004**, *104* (10), 4303-4417.

14. Aurbach, D.; Schechter, A. Changes in the resistance of electrolyte solutions during contact with lithium electrodes at open circuit potential that reflect the Li surface chemistry. *Electrochim. Acta* **2001**, *46* (15), 2395-2400.

15. Xiao, L. F.; Cao, Y. L.; Ai, X. P.; Yang, H. X. Optimization of EC-based multi-solvent electrolytes for low

temperature applications of lithium-ion batteries. *Electrochim. Acta* **2004**, *49* (27), 4857-4863.

16. Quartarone, E.; Tomasi, C.; Mustarelli, P.; Appetecchi, G. B.; Croce, F. Long-term structural stability of PMMA-based gel polymer electrolytes. *Electrochim. Acta* **1998**, *43* (10-11), 1435-1439.

17. Zhang, S. S.; Jow, T. R.; Amine, K.; Henriksen, G. L. $LiPF_6$–EC–EMC electrolyte for Li-ion battery. *J. Power Sources* **2002**, *107* (1), 18-23.

18. Botte, G. G.; White, R. E.; Zhang, Z. Thermal stability of $LiPF_6$-EC:EMC electrolyte for lithium ion batteries. *J. Power Sources* **2001**, *97-98* (0), 570-575.

19. Ding, M. S.; Xu, K.; Zhang, S. S.; Amine, K.; Henriksen, G. L.; Jow, T. R. Change of conductivity with salt content, solvent composition, and temperature for electrolytes of $LiPF_6$ in ethylene carbonate-ethyl methyl carbonate. *J. Electrochem. Soc.* **2001**, *148* (10), A1196-A1204.

20. Plichta, E. J.; Hendrickson, M.; Thompson, R.; Au, G.; Behl, W. K.; Smart, M. C.; Ratnakumar, B. V.; Surampudi, S. Development of low temperature Li-ion electrolytes for NASA and DoD applications. *J. Power Sources* **2001**, *94* (2), 160-162.

21. Plichta, E. J.; Behl, W. K. A low-temperature electrolyte for lithium and lithium-ion batteries. *J. Power Sources* **2000**, *88* (2), 192-196.

22. Herreyre, S.; Huchet, O.; Barusseau, S.; Perton, F.; Bodet, J. M.; Biensan, P. New Li-ion electrolytes for low temperature applications. *J. Power Sources* **2001**, *97-98*, 576-580.

23. Azeez, F.; Fedkiw, P. S. Conductivity of libob-based electrolyte for lithium-ion batteries. *J. Power Sources* **2010**, *195* (22), 7627-7633.

24. Ein-Eli, Y.; Thomas, S. R.; Koch, V.; Aurbach, D.; Markovsky, B.; Schechter, A. Ethylmethylcarbonate, a promising solvent for li-ion rechargeable batteries. *J. Electrochem. Soc.* **1996**, *143* (12), L273-L277.

25. Smart, M. C.; Ratnakumar, B. V.; Whitcanack, L. D.; Chin, K. B.; Surampudi, S.; Croft, H.; Tice, D.; Staniewicz, R. Improved low-temperature performance of lithium-ion cells with quaternary carbonate-based electrolytes. *J. Power Sources* **2003**, *119–121*, 349-358.

26. Kang, H.; Wang, G.; Guo, H.; Chen, M.; Luo, C.; Yan, K. Facile Synthesis and Electrochemical Performance of $LiFePO_4$/C Composites Using Fe–P Waste Slag. *Ind. Eng. Chem. Res.* **2012**, *51* (23), 7923-7931.

27. Wang, G.; Yan, K.; Yu, Z.; Qu, M. Facile synthesis and high rate capability of $Li_4Ti_5O_{12}$/C composite materials with controllable carbon content. *J. Appl. Electrochem.* **2010**, *40* (4), 821-831.

28. Liao, X. Z.; Ma, Z. F.; He, Y. S.; Zhang, X. M.; Wang, L.; Jiang, Y. Electrochemical behavior of $LiFePO_4$/C cathode material for rechargeable lithium batteries. *J. Electrochem. Soc.* **2005**, *152* (10), A1969-A1973.

29. Macdonald, J. Impedance spectroscopy. *Ann. Biomed. Eng.* **1992**, *20* (3), 289.

30. Liu, H.; Li, C.; Zhang, H. P.; Fu, L. J.; Wu, Y. P.; Wu, H. Q. Kinetic Study on $LiFePO_4$/C nanocomposites synthesized by solid state technique. *J. Power Sources* **2006**, *159* (1), 717-720.

31. Rho, Y. H.; Kanamura, K. Li^+ ion diffusion in $Li_4Ti_5O_{12}$ thin film electrode prepared by PVP sol-gel method. *J. Solid State Chem.* **2004**, *177* (6), 2094-2100.

32. A.Y. Shenouda, H.K. Liu, Preparation, characterization, and electrochemical performance of Li2CuSnO4 and $Li_2CuSnSiO_6$ electrodes for lithium batteries, *Journal of The Electrochemical Society* **2010**, *157,* A1183-A1187.

33. F. Nobili, M. Mancini, P. E. Stallworth, F. Croce, S. G. Greenbaum, R. Marassi,. Tin-coated graphite electrodes as composite anodes for Li-ion batteries. Effects of tin coatings thickness toward intercalation behavior. *Journal of Power Sources* **2012**, *198,* 243-250.

Table Captions

Table 1. Compositions of various electrolytes.

Table 2. Physical properties of selected aprotic solvents at 25 °C.

Table 3. Discharge capacities (mAh g $^{-1}$), η (%), and ΔV (V) of LiFePO$_4$/C composite at 0.1 C using

different electrolytes under various temperatures.

Table 4. E_O, E_R, ΔE, I_O and I_R of LiFePO$_4$/C composite using different electrolytes at -20 °C.

Table 5. R_s, R_ct and R_f of LiFePO$_4$/C composite using different electrolytes under various temperatures.

Table 6. σ, D_Li, j and E_a of LiFePO$_4$/C composite using different electrolytes under various

temperatures.

Tables

Table 1. Compositions of various electrolytes.

Electrolyte [*]	EC : DMC : EMC: EA (Volume ratio)
"1"	30:50:20:0
"2"	30:20:50:0
"3"	30:20:30:20

[*] All contain 2 wt.% VC.

Table 2. Physical properties of selected aprotic solvents at 25 °C.

Solvent	EC	DMC	EMC	EA	VC
Structure	22	/	C	22	22
Viscosity (10^{-3} Pa·s)	1.93 (40 °C)	0.59	0.65	0.46	1.9 (40 °C)
Dielectric constant, ε	89.60	3.10	2.40	6.02	96
Melting point (°C)	39	4.60	-55	-84.00	22
Boiling point (°C)	248	90	108	71.10	162
Flash point (°C)	160	18	26.7	-3	73
Density (g cm^{-3})	1.32 (39 °C)	1.06	1.01	0.89	1.36
Dipole moment (debye)	4.61	0.76	0.89	--	--
Donor number	16.40	15.10	--	17.10	--

Table 3. Discharge capacities (mAh g^{-1}), η (%), and ΔV (V) of LiFePO$_4$/C composite at 0.1 C using

different electrolytes under various temperatures.

Electrolyte	20 °C			0 °C			-20 °C		
	Capacity	η	ΔV	Capacity	η	ΔV	Capacity	η	ΔV
"1"	140.4	99.4	0.065	96.2	98.0	0.07	77.5	91.4	0.15
"2"	144.9	99.8	0.051	98.9	100	0.17	78.4	95.0	0.17
"3"	131.8	97.8	0.056	99.4	97.5	0.14	86.0	99.2	0.10

Table 4. E_O, E_R, ΔE, I_O and I_R of LiFePO$_4$/C composite using different electrolytes at -20 °C.

Electrolyte	E_O(V)	E_R(V)	ΔE (V)	I_O (mA cm^{-2})	I_R (mA cm^{-2})
"1"	3.75	3.15	0.60	0.48	-0.42
"2"	3.79	3.20	0.59	0.63	-0.50
"3"	3.74	3.21	0.53	0.71	-0.56

Table 5. R_s, R_{ct} and R_f of LiFePO$_4$/C composite using different electrolytes under various temperatures.

Electrolyte	20°C			0°C			-20°C		
	R_s(ohm)	R_{ct}(ohm)	R_f(ohm)	R_s(ohm)	R_{ct}(ohm)	R_f(ohm)	R_s(ohm)	R_{ct}(ohm)	R_f(ohm)
"1"	1.4	45.7	3.6	4.3	270.0	4.2	6.4	874.7	28.7
"2"	2.2	71.4	6.9	11.0	306.2	15.5	11.6	560.8	30.4
"3"	1.6	73.3	2.6	13.1	297.2	3.1	13.6	513.2	18.5

Table 6. σ, D_{Li}, j and E_a of LiFePO$_4$/C composite using different electrolytes under various

temperatures.

| Electrolyte	Temperature (°C)	σ	D_{Li} (cm^2 s^{-1})	J (A cm^{-2})	E_a (kJ mol^{-1})
"1"	20	9.58	2.88×10^{-10}	4.48×10^{-4}	
	0	22.76	4.41×10^{-11}	7.76×10^{-5}	48.36
	-20	87.35	2.62×10^{-12}	2.20×10^{-5}	
"2"	20	9.05	3.22×10^{-10}	3.13×10^{-4}	
	0	22.76	4.42×10^{-11}	6.79×10^{-5}	33.29
	-20	80.10	3.11×10^{-12}	3.80×10^{-5}	
"3"	20	9.25	3.12×10^{-10}	3.04×10^{-4}	
	0	17.03	6.88×10^{-11}	7.00×10^{-5}	33.01
	-20	28.26	2.50×10^{-11}	3.75×10^{-5}	

Figure Captions

Figure 1. XRD pattern of the as-synthesized LiFePO$_4$/C composite.

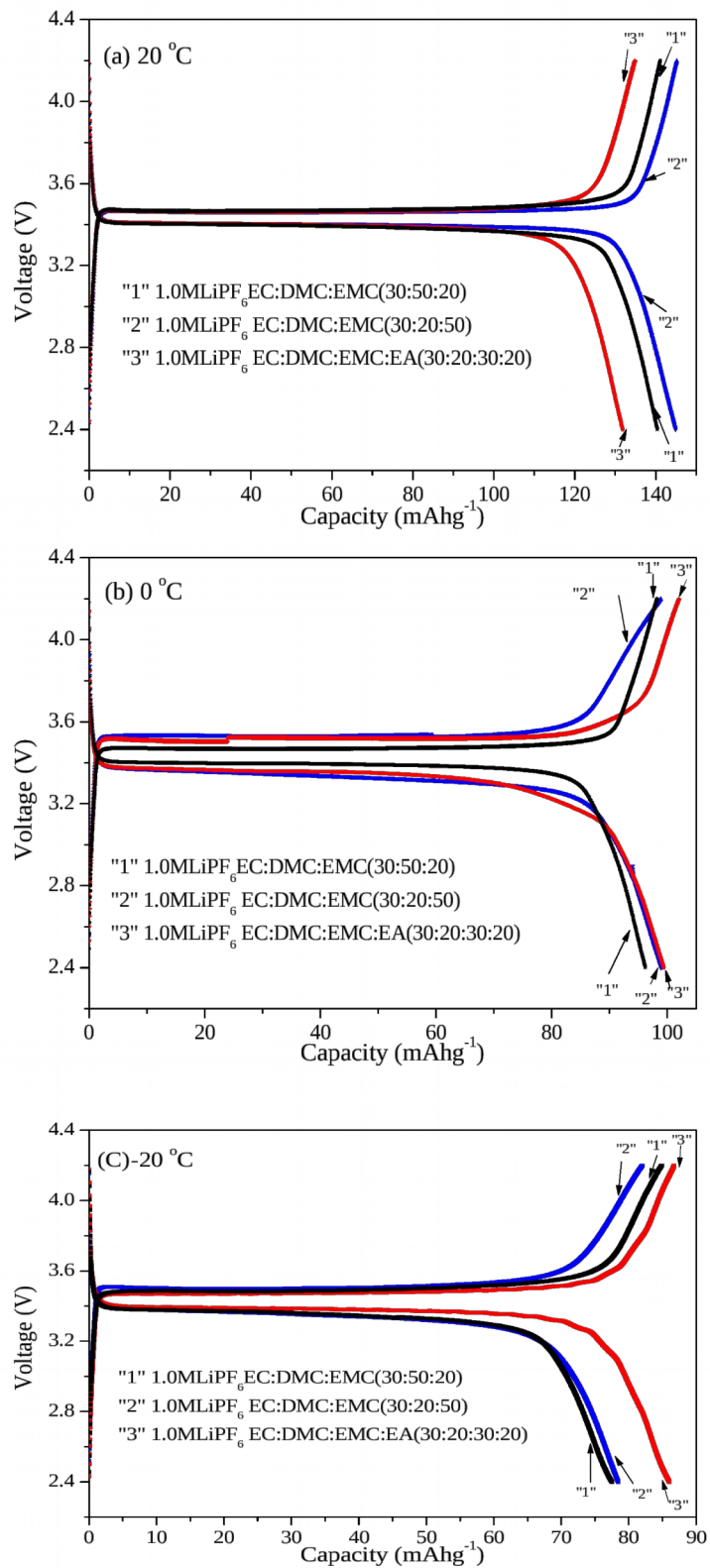Figure 2. SEM images of the as-synthesized LiFePO$_4$/C composite.

Figure 3. Galvanostatic charge/discharge curves of LiFePO$_4$/C composite using different electrolytes under various temperatures.
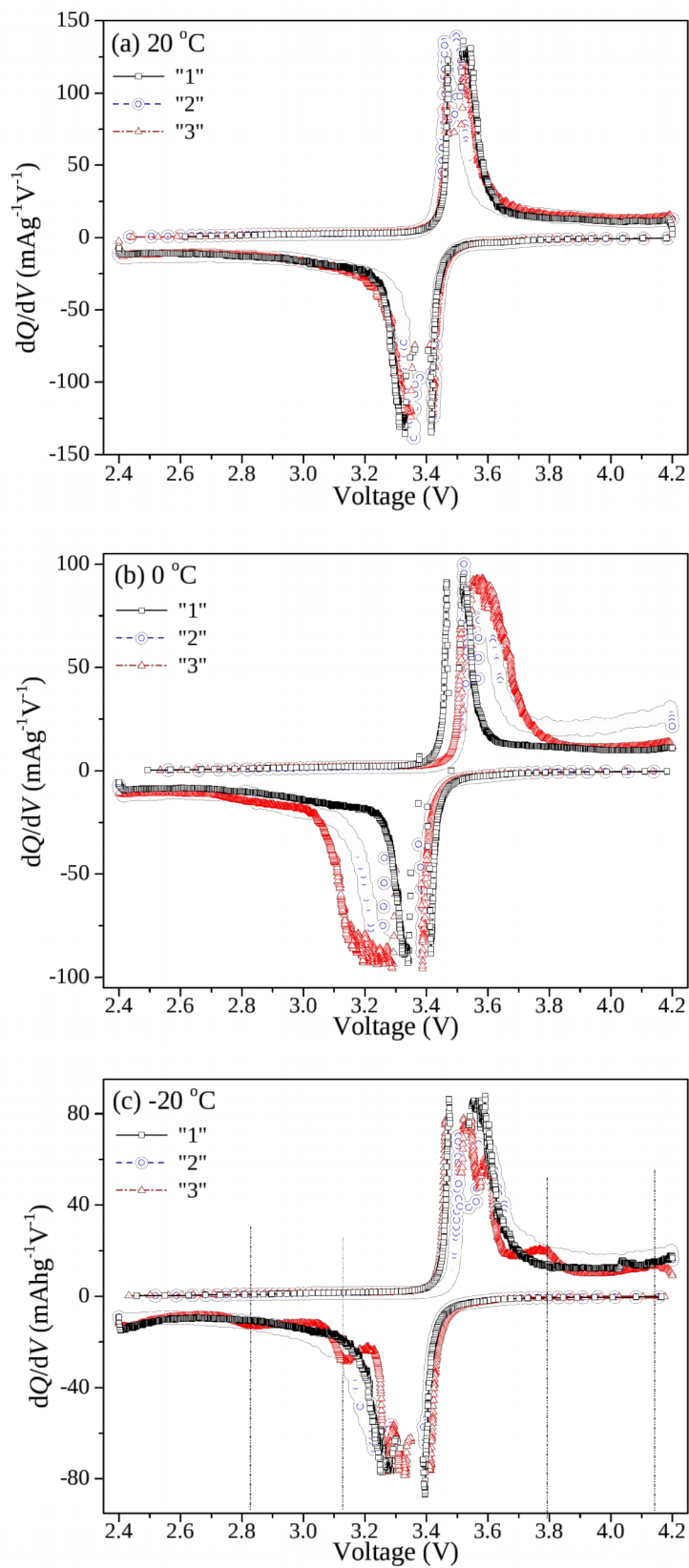
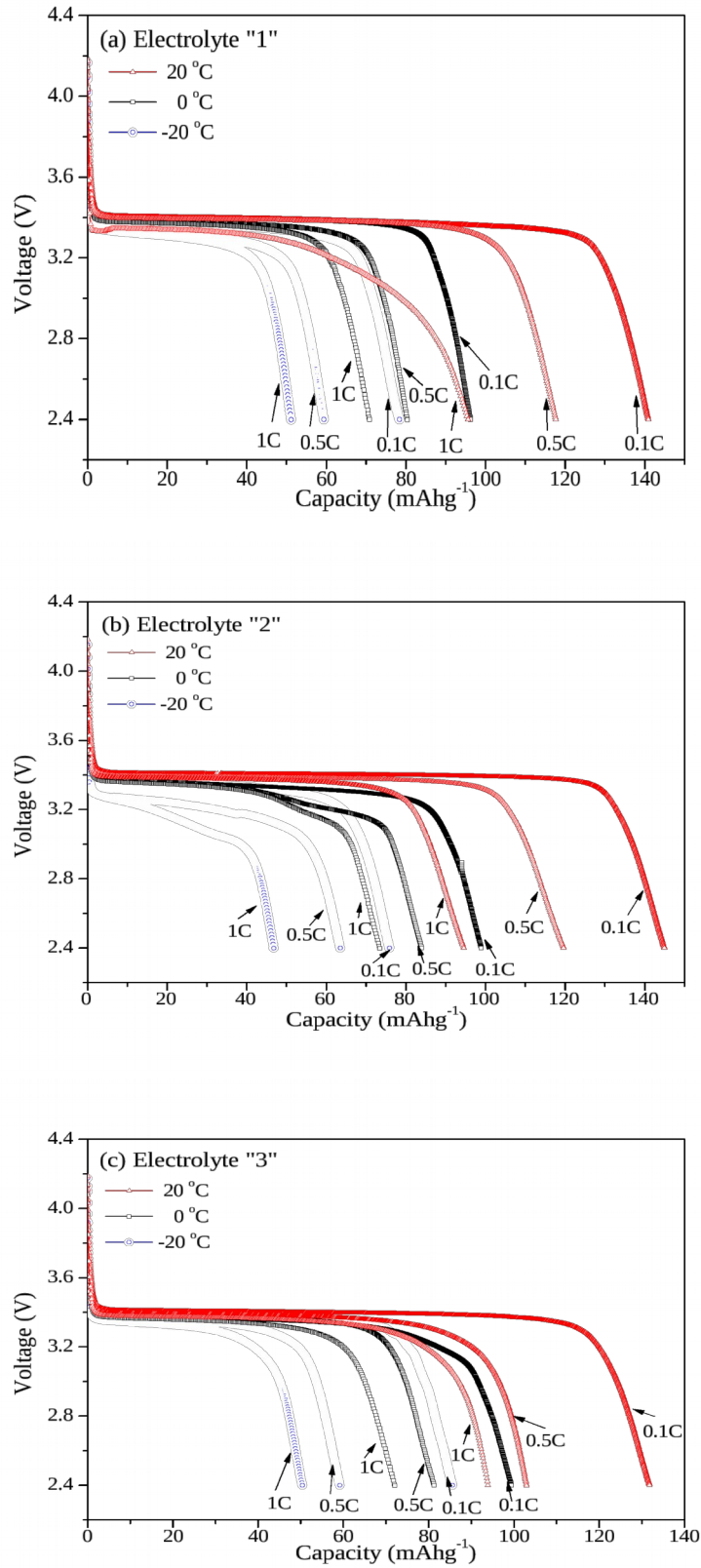Figure 4. Differential capacity plots of the data shown in Figure 3.

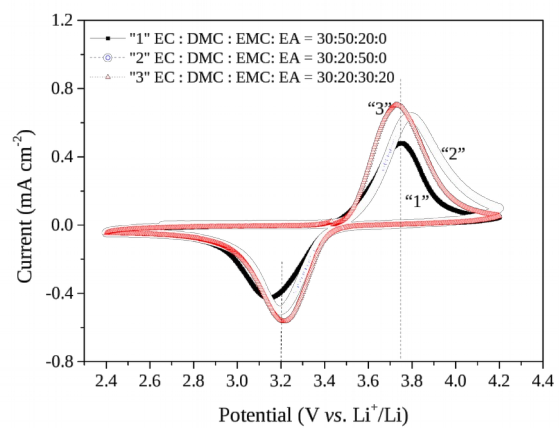Figure 5. Influence of electrolyte on the rate performance of LiFePO$_4$/C composite under different temperatures.

Figure 6. Cyclic voltammograms of LiFePO$_4$/C composite using various electrolytes at -20 °C.
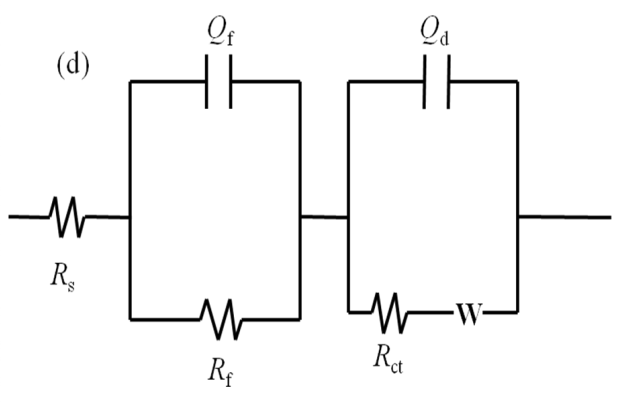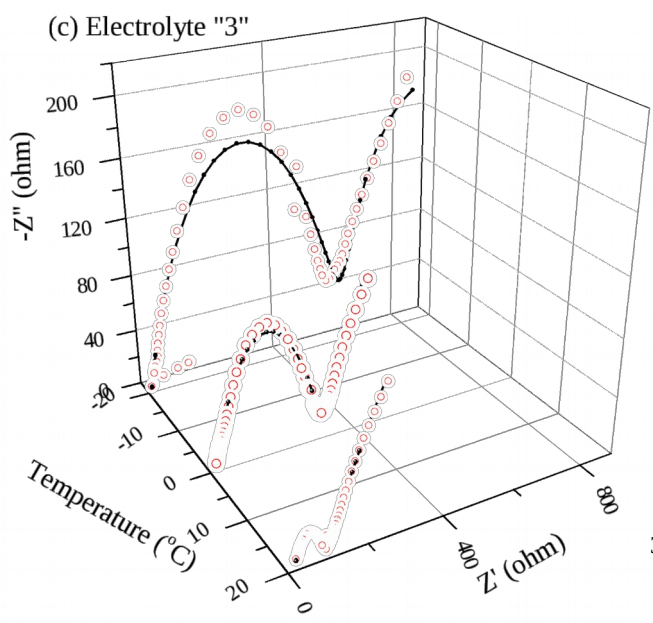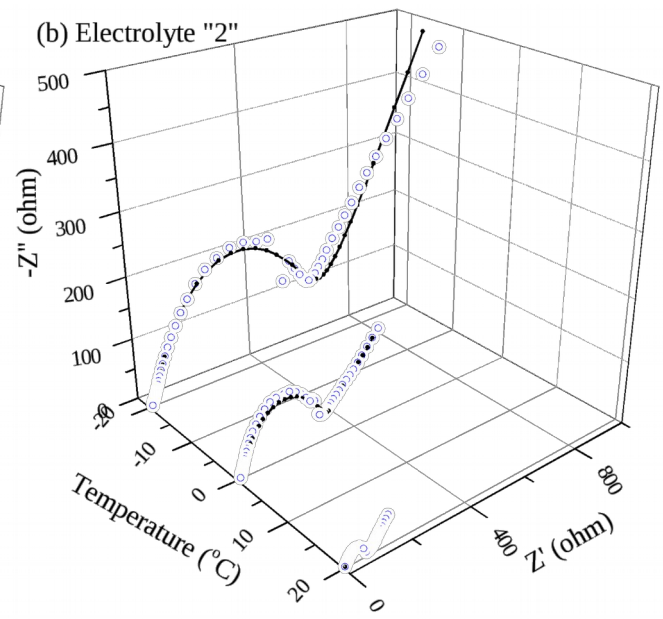
Figure 7. Nyquist plots of LiFePO$_4$/C composite under different temperatures with various electrolytes (a) "1", (b) "2", (c) "3", and (d) corresponding equivalent circuit.

Figure 8. *Z' vs. ω$^{-1/2}$* of LiFePO$_4$/C composite with various electrolytes under different temperatures.

Figure 9. Influence of temperature and electrolyte on the chemical diffusion coefficient of lithium ions.

Figures
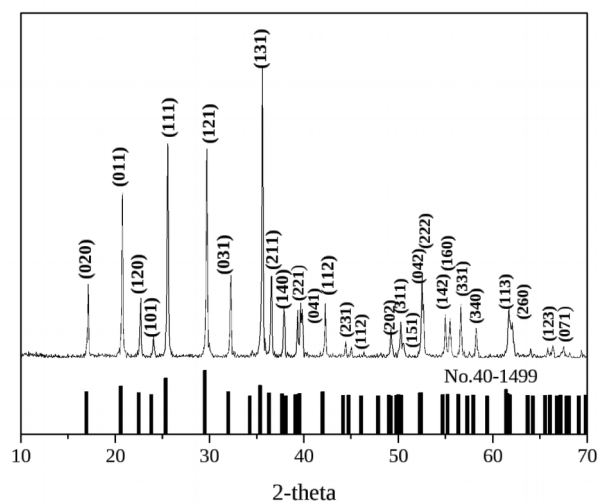
Figure 1. XRD pattern of the as-synthesized LiFePO₄/C composite.

Figure 2. SEM images of the as-synthesized LiFePO₄/C composite.

Figure 3. Galvanostatic charge/discharge curves of LiFePO$_4$/C composite using various electrolytes under different temperatures.

Figure 4. Differential capacity plots of the data shown in Fig. 2.

Figure 5. Influence of electrolyte on the rate performance of LiFePO₄/C composite under different temperatures.

Figure 6. Cyclic voltammograms of LiFePO$_4$/C composite using various electrolytes at -20°C.
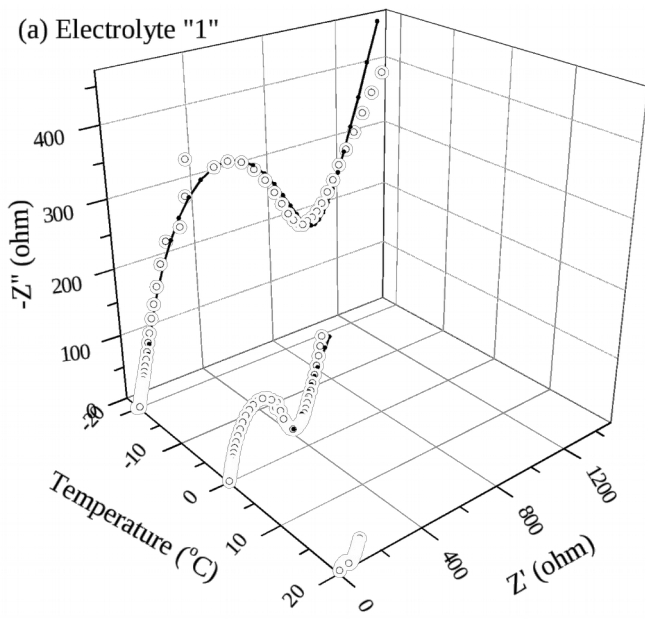
(a) Electrolyte "1"

(b) Electrolyte "2"

(c) Electrolyte "3"

(d)

Q_f

Q_d

R_s

R_f

R_ct

W

33

Figure 7. Nyquist plots of LiFePO$_4$/C composite under different temperatures using various electrolytes (a) "1", (b) "2", (c) "3", and (d) corresponding equivalent circuit. The experiment data are shown in open circle, and the fitting data are shown in black line.
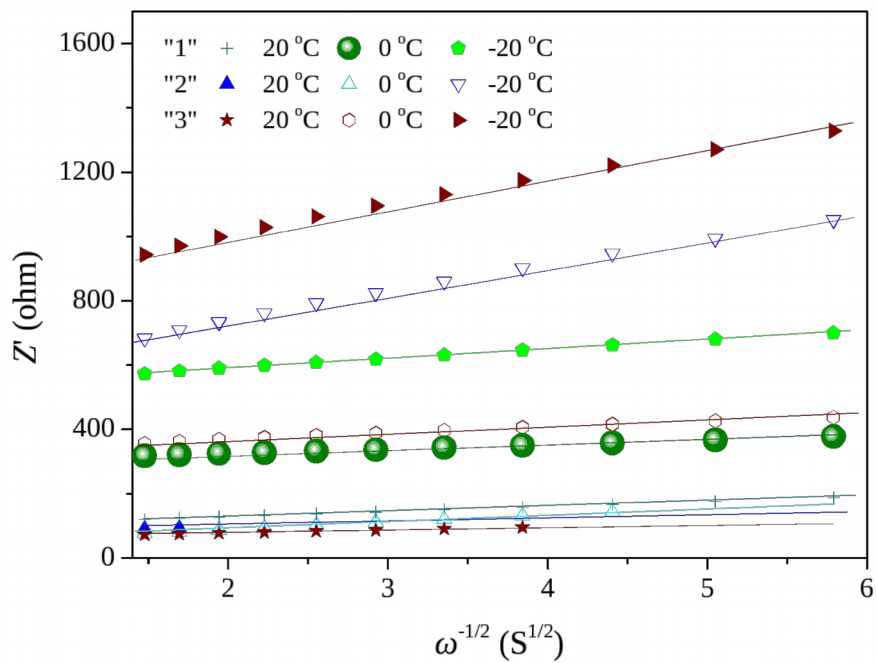

Figure 8. *Z' vs. ω*$^{-1/2}$ of LiFePO$_4$/C composite using various electrolytes under different temperatures.
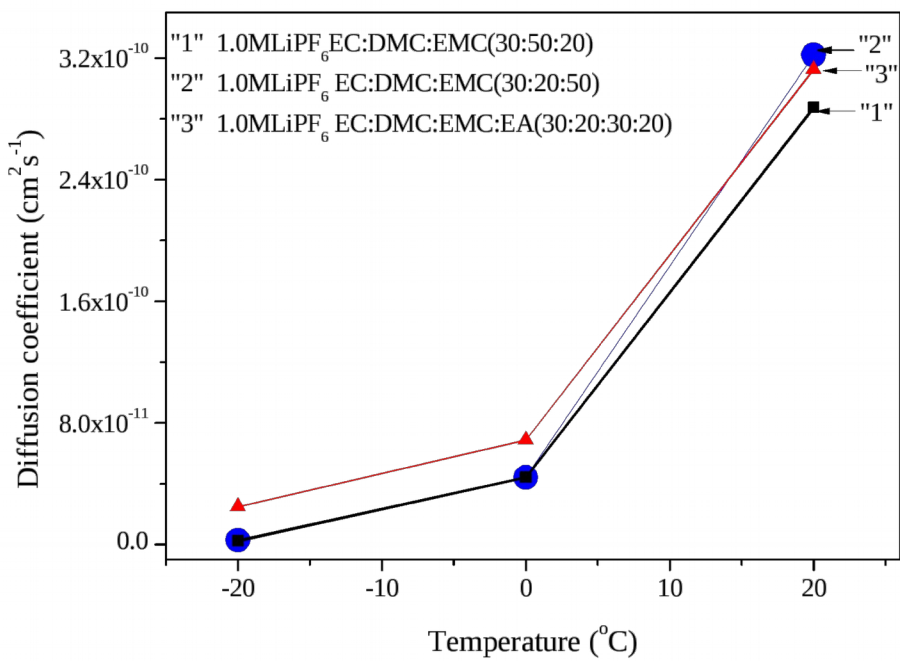
Figure 9. Influence of temperature and electrolyte on the chemical diffusion coefficient of lithium ions.